# Quasi-Linear Analysis Of Anomalous Electron Mobility Inside A Hall Thruster

**IEPC-2007-70**

*Presented at the* $30^{th}$ *International Electric Propulsion Conference, Florence, Italy*
*September 17-20, 2007*

Rostislav Spektor*

**A quasi-linear plasma model is used to investigate anomalous electron mobility, caused by electrostatic fluctuations, inside a Hall thruster. The model calculates effective anomalous electron collision frequency $\nu_{AN}$ from plasma susceptibility, which is computed from the fluid dispersion relation. The dispersion relation takes into account axial gradients in the steady-state electric and magnetic fields, plasma density, as well as electron temperature. Additionally, the dispersion relation allows waves to propagate perpendicularly to the magnetic field at an arbitrary angle in the $z-\theta$ plane.**

## Nomenclature

$n$ = plasma density
$v$ = velocity
$E$ = electric field
$B$ = magnetic field
$T$ = temperature
$\nu$ = collision frequency
$\chi$ = susceptibility
$k$ = wavenumber
$\omega$ = wave frequency
$m$ = particle mass
$q$ = particle charge
$\omega_c$ = particle cyclotron frequency
$\omega_p$ = plasma frequency
$\mu$ = mobility

*Member of Technical Staff, The Aerospace Corporation, rostislav.spektor@aero.org

# I. Introduction

Hall thrusters are space plasma propulsion devices that rely on axial electric field to accelerate ions. Electric field profile, $E_z(z)$, inside the thruster is established by electrons, which flow from the external cathode to the anode, and are trapped in the annular discharge channel by applied radial magnetic field, $B_r(z)$, long enough to ionize propellant gas. The combination of the axial electric and radial magnetic fields results in primarily azimuthal electron drift proportional to $E_z/B_r$. The axial, or cross-field, electron flow depends on collision frequency with heavy species, thruster walls, and propagating electromagnetic fluctuations. Electron transport plays critical role in thruster operation.

One puzzling finding coming from both experimental as well as numerical investigations of electron transport in Hall thrusters was higher than expected cross-field electron current in the region close to the thruster exit.[1–5] Phenomenon of anomalous electron cross-field transport is not confined exclusively to the Hall thruster geometry. Similar electron behavior has been observed in high temperature, fusion type plasmas with crossed electric and magnetic fields, and in presence of various gradients.[6–8] Unfortunately, the fundamental nature of the anomalous transport mechanism has not been fully uncovered. Two major schools of thought have emerged to explain this phenomenon. One explanation, advocated by Morozov *et al*.[9] relies on the enhanced near-wall mobility. Another theory advanced to explain the high electron cross-field mobility invokes turbulent transport.

The problem of turbulent cross-field transport has been studied in details by many authors. Most notable is a series of work reported by Krall *et al*.[10–12] related to fusion-type devices. The authors of that work have used the quasi-linear kinetic approach to derive an expression for the electron anomalous collision frequency. Similar approach has been taken by Choueiri[13,14] to derive anomalous resistivity in the MPD thrusters. A first step in applying the quasi-linear theory to the problem of anomalous cross-field electron mobility in Hall thrusters has been taken by Thomas and Cappelli,[15] who have used the fluid flow approximation to derive a simple dispersion relation for the Hall thruster plasma.

In this paper we adopt the approach developed by Krall *et al*. to investigate anomalous electron transport in Hall thrusters. We expand on the work presented in Ref. [15] by deriving a generalized dispersion relation that takes into account electron temperature, axial gradients in the electric and magnetic fields, plasma density, as well as the ion and electron velocities. Gradient formulation is left in the most general form, thus allowing the use of either experimentally determined steady-state profiles, or those found through numerical simulation. This generalized dispersion relation, when solved, allows a more accurate expression of the anomalous mobility inside a Hall thruster.

The paper is organized as follows. In Section II we briefly describe how the quasi-linear approach can be applied to the problem of anomalous cross-field electron transport, and provide an expression for the anomalous collision frequency. In the next two sections we discuss general expressions for electron motion, and derive the fluid dispersion relation. We then show in Section V that in a limiting case this generalized dispersion relation leads to a well-known expression. Finally, in Section VI we compute the anomalous collision frequency for two sample cases.

# II. Quasi-linear Theory

The quasi-linear approach applied to the problem of anomalous cross-field electron transport relies on perturbation analysis of the Vlasov equation, as described in numerous works, such as by Liewer and Krall[11] or Choueiri.[13] We will not reproduce these derivations here, but simply state that the perturbation analysis leads to the following set of fluid equations for any charged species $\alpha$

$$\frac{\partial n_\alpha}{\partial t} + \nabla \cdot n_\alpha \vec{v_\alpha} = 0, \tag{1a}$$

$$\frac{\partial n_\alpha \vec{v_\alpha}}{\partial t} + \nabla n_\alpha \vec{v_\alpha} \vec{v_\alpha} = \frac{q_\alpha n_\alpha}{m_\alpha}\left(\vec{E} + \vec{v_\alpha} \times \vec{B}\right) - \frac{1}{m_\alpha}\nabla n_\alpha T_\alpha - \nu_\alpha n_\alpha \vec{v_\alpha} + \frac{q_\alpha}{m_\alpha} < n_\alpha^1 \vec{E^1} >, \tag{1b}$$

where besides the last term in the second equation, the set is easily recognized as the fluid mass and momentum conservation equations. Here, as usual, $m_\alpha$, $q_\alpha$, $n_\alpha$, and $\vec{v}_\alpha$ are the mass, charge, density, and velocity, while $\vec{E}$ and $\vec{B}$ are the electric and magnetic fields, $T_\alpha$ is the temperature, and $\nu_\alpha$ is the collisions frequency. Similarly, one can derive the energy conservation equation. We now use these two equations to investigate electron transport. Two underlying limitations already imposed on this model are: 1) electrons are in isotropic equilibrium, i.e. their velocity distribution is Maxwellian, and 2) perturbation wavelength is small as compared to variations in macroscopic plasma properties, i.e. $k^{-1} \ll \partial/\partial x$.

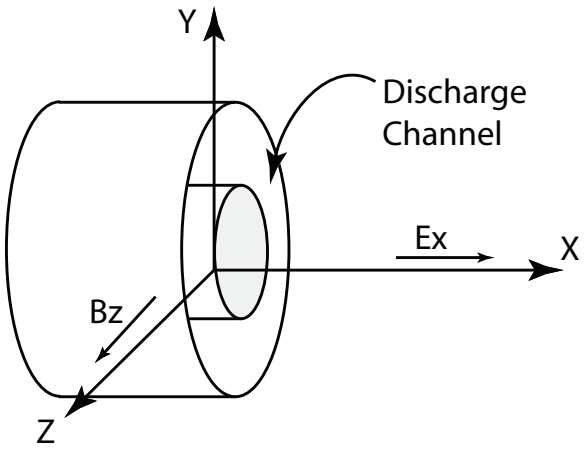


**Figure 1. Schematic of a Hall thruster showing the coordinate system in the plasma-slab approximation.**

There is some evidence that electron energy distribution function inside Hall thrusters is not Maxwellian.[16–19] The non-Maxwellian distribution may affect the cross-field transport, by acting as a source of plasma instabilities. Furthermore, kinetic fluctuations may interact stronger with electrons than the fluid modes, because kinetic modes tend to have a shorter wavelength – on the order of the electron Larmor radius. In this paper we only examine fluid fluctuations. The fluid approach has been adopted as a first simplifying step in the anomalous transport analysis, and examination of possible kinetic effects is left for future work. We also restrict our investigation to purely electrostatic fluctuations. In the low-beta plasmas, such as the Hall thruster discharge, electromagnetic modes result in a small correction to the electrostatic analysis.

The last term in Eq. (1b) is the momentum transport contribution due to the fluctuating field. It can be shown[13] that this quantity can be expressed in terms of the anomalous collision frequency $\nu_{AN}$, which is the effective rate of interaction between the electrons and the fluctuations,

$$\begin{aligned} \left.\frac{\partial n^0 \vec{v}_e^0}{\partial t} \cdot \vec{v}_e^0\right|_{AN} &= -\nu_{AN} n^0 \vec{v}_e^0 \cdot \vec{v}_e^0 = -\frac{e}{m_e} < n_e^1 \vec{E}^1 > \cdot \vec{v}_e^0 = -2 \int d\vec{k} \mathrm{Im}[\vec{k} \cdot \chi_e] \cdot \vec{E}_{\vec{k}} \Rightarrow \\ \Rightarrow \quad \nu_{AN} &\approx \frac{2\mathcal{E}}{n^0 m_e (v_e^0)^2} \mathrm{Im}[\vec{k} \cdot \vec{v}_e^0 \chi_i]\Big|_{\omega(\vec{k})}, \end{aligned} \tag{2}$$

where $\chi$ is the plasma susceptibility, $\vec{E}_{\vec{k}}$ is the Fourier-transformed field amplitude, and $\mathcal{E}$ is the saturation energy of the wave. There are multiple saturation mechanisms. A good discussion of these mechanisms is given, for example, by Choueiri.[13] In this work, we assume that fluctuation energy saturates through the electron motion, and thus we adopt the Fowler's thermodynamic limit, $\mathcal{E} \approx \frac{1}{2} n_e m_e (v_e^0)^2$.

Furthermore, in the expression above we have substituted the electron susceptibility $\chi_e$ by ion susceptibility $\chi_i$ since the dispersion relation can be expressed as $1 + \chi_e + \chi_i = 0$, and therefore $\mathrm{Im}[\chi_e] = -\mathrm{Im}[\chi_i]$. Expression (2) implies that the anomalous collision frequency should be evaluated with $\omega(\vec{k}) = \omega_r + i\omega_i$, which is the solution to the dispersion relation.

## III. Electron Mobility

We now adopt the equation set (1) to the Hall thruster geometry, as shown in Fig. 1. Here we assume a plasma slab geometry, in which the $y$ axis corresponds to $\theta$ direction, $z$ axis corresponds to the radial direction, and $x$ axis corresponds to the axial direction. Thus, the applied radial magnetic field is $B_z^0$, and the axial electric field is $E_x^0$ – the "0" superscript signifying a steady-state quantity.

Expressing Eq. (1b) for the steady-state electron transport we get

$$v_{ex}^0 = \frac{-1}{\nu_e(1 + \omega_{ce}^2/\nu_e^2)} \left( \frac{e}{m_e} E_x^0 + \frac{1}{m_e n_e} \frac{\partial n_e^0 T_e^0}{\partial x} \right), \tag{3a}$$

$$v_{ey}^0 = \frac{\omega_{ce}}{\nu_e} v_{ex}^0, \tag{3b}$$

where $\nu_e = \nu_c + \nu_{AN}$ is the combined classical $\nu_c$ and anomalous $\nu_{AN}$ electron collision frequency. In the following derivation, however, we will ignore the anomalous contribution to Eq. (3). Including this term requires an iterative process, where the anomalous collision frequency is calculated first with the classical quantities by the process described below, then substituting the computed value of $\nu_{AN}$ into Eq. (3), and repeating the calculation. We can now define the cross-field mobility as

$$\mu_\perp = \frac{n_e^0 e^2}{m_e \nu_e} \frac{1}{(1 + \omega_{ce}^2/\nu_e^2)}, \tag{4}$$

where, in the absence of the anomalous transport, the equation above leads to the well-known classical behavior: $\mu_\perp \sim 1/B^2$.

## IV. Dispersion Relation

In order to obtain an expression for $\nu_{AN}$ relevant to the Hall thruster geometry we need to solve a dispersion relation, which reflects realistic conditions in the thruster discharge. While, we do not solve the full kinetic dispersion relation, in this work we include many factors, such as velocity, field, density, and temperature gradients, which play an important role in establishing the steady-state and transient plasma properties in the discharge. We start by rewriting the continuity and momentum conservation equations for electrons.

$$\frac{\partial n_e}{\partial t} + \nabla \cdot n\vec{v_e} = 0, \tag{5a}$$

$$\frac{\partial n_e \vec{v_e}}{\partial t} + \nabla n_e \vec{v}_e \vec{v}_e = \frac{e n_e}{m_e}\big(\vec{E} + \vec{v}_e \times \vec{B}\big) - \frac{1}{m_e}\nabla n_e T_e - \nu_e n_e \vec{v}_e. \tag{5b}$$

We then assume that gradients in $z$ and $y$ direction are negligible, and linearize the appropriate parameters as follows,

$$\vec{v}_e = \vec{v}_e^0 + \vec{v}_e^1, \quad n_e = n_e^0 + n_e^1, \quad \text{and} \quad \vec{B} = B_z^0(x), \quad \vec{E} = E_x^0(x) + \vec{E}^1. \tag{6}$$

We also assume that the first-order components are periodic, $e^{-(\vec{k}\cdot r - \omega t)}$, and are free to propagate in $x$ and $y$ direction. With this linearization we get a set of the first-order equations

$$i\omega n_e^1 - i\vec{k}\cdot\vec{v}_e^0 n_e^1 - i\vec{k}\cdot\vec{v}_e^1 n^0 + n_e^1 \nabla\cdot\vec{v}_e^0 + \vec{v}^1\cdot\nabla n^0 = 0, \tag{7a}$$

$$i\omega\vec{v}_e^1 - (\vec{v}^0\cdot\vec{k})\vec{v}_e^1 + (\vec{v}^1\cdot\nabla)\vec{v}_e^0 = -\frac{e}{m_e} i\vec{k}\Phi^1 - \vec{v}_e^1 \times \omega_{ce} - \nu_e \vec{v}_e + \frac{T_e^0}{m_e n_e^0}\left(i\vec{k} n_e^1 + n_e^1 \frac{\nabla n^0}{n^0}\right), \tag{7b}$$

where we have used the binomial expansion to simplify $\nabla n_e T_e$ as

$$\frac{1}{n_e}\nabla n_e T_e = \nabla T_e + \frac{T_e}{n_e} \approx \frac{T_e^0}{n^0 + n_e^1}\nabla(n^0 + n_e^1) = T_e^0\left(-\frac{n^1}{(n^0)^2}\nabla n^0 + \frac{\nabla n^1}{n^0}\right). \tag{8}$$

We can now further simplify the continuity equation, and write down the $x$ and $y$ components of the first-order momentum equation

$$n_e^1(\omega - \vec{k}\cdot\vec{v}_e^0 - i\nabla\cdot\vec{v}_e^0) = \vec{v}_e^1\cdot(\vec{k} + i\nabla)n^0, \tag{9a}$$

$$v_{ex}^1\left(\omega - \vec{k}\cdot\vec{v}_e^0 - i\nu_e - i\frac{\partial v_{ex}^0}{\partial x}\right) = -\frac{e}{m_e}k_x\Phi^1 + i v_{ey}^1\omega_{ce} + \frac{T_e^0}{m_e n^0}\left(k_x n_e^1 - i\frac{n_e^1}{n^0}\frac{\partial n^0}{\partial x}\right), \tag{9b}$$

$$v_{ey}^1\left(\omega - \vec{k}\cdot\vec{v}_e^0 - i\nu_e\right) = -\frac{e}{m_e}k_y\Phi^1 - i v_{ex}^1(\omega_{ce} - \frac{\partial v_{ey}^0}{\partial x}) + \frac{T_e^0}{m_e n^0}\left(k_y n_e^1 - i\frac{n_e^1}{n^0}\frac{\partial n^0}{\partial y}\right). \tag{9c}$$

In the equations above we maintained $\nabla$ to signify the gradients for convenience, but it is important to remember that the non-zero gradients are only in $x$ direction. The set of equations above suggests the following expressions for $n_e^1$ and $v_e^1$ in vector notation

$$n_e^1 = \frac{\vec{v}_e^1\cdot(\vec{k} + i\nabla)n_e^0}{a_e + i\nu_e} \tag{10a}$$

$$\vec{v}_e^1 = -\frac{e}{m_e}k_x\Phi^1\frac{A_e\cdot\vec{k}}{\det A_e} + \frac{n_e^1 T_e^0}{m_e n^0}\left(\frac{A_e\cdot\vec{k}}{\det A_e} - i\frac{A_e\cdot\nabla n^0}{n^0 \det A_e}\right), \tag{10b}$$

where $A_e$ is a $2 \times 2$ matrix with elements,

$$A_e = \begin{bmatrix} b_e & -c_e \\ d_e & a_e \end{bmatrix}, \quad \text{with} \tag{11}$$

$$a_e = b_e - i\frac{\partial v_{ex}^0}{\partial x}, \quad b_e = \omega - \vec{k}\cdot\vec{v}_e^0 - i\nu_e, \quad c_e = -i\omega_{ce}, \quad d_e = c_e + i\frac{\partial v_{ey}^0}{\partial x}. \tag{12}$$

We should note that expressions $A_e \cdot \vec{k}$ and $A_e \cdot \nabla n^0$ should each be treated like a single vector rather than an inner product of two separate quantities. For example,

$$A_e \cdot \vec{k} = (k_x b_e - k_y c_e)\hat{x} + (k_x d_e + k_y a_e)\hat{y}. \tag{13}$$

To emphasize this fact in the derivation below, we enclose these entities in parentheses. Using expression for $v_e^1$ we now express $n_e^1$ as follows,

$$n_e^1 = -\frac{\frac{e}{m_e}\Phi^1(A_e\cdot\vec{k})\cdot(\vec{k}+i\nabla)n^0/\left[(a_e+i\nu_e)\det A_e\right]}{\left[1-\frac{T_e^0}{m_e n^0}\frac{1}{(a_e+i\nu_e)\det A_e}\left\{(A_e\cdot\vec{k})\cdot(\vec{k}+i\nabla)n^0 - \frac{1}{n^0}\left[(iA_e\cdot\nabla n^0)\cdot(\vec{k}+i\nabla)n^0\right]\right\}\right]} \tag{14}$$

Expression for the ion density $n_i^1$ is obtained by replacing subscript $e$ by $i$ in Eq. (14), and remembering that ions are not-magnetized ($B = 0$), cold ($T_i = 0$), and collisionless ($\nu_i = 0$). Then, expression for $n_i^1$ reduces to

$$n_i^1 = \frac{e}{m_i}\Phi^1\frac{(A_i\cdot\vec{k})}{a_i\det A_i}\cdot(\vec{k}+i\nabla)n^0, \tag{15}$$

where matrix $A_i$ is now

$$A_i = \begin{bmatrix} b_i & 0 \\ 0 & a_i \end{bmatrix}, \quad \text{with} \tag{16}$$

$$a_i = b_i - i\frac{\partial v_{ix}^0}{\partial x}, \quad b_e = \omega - \vec{k}\cdot\vec{v}_i^0. \tag{17}$$

Using the Poisson equation we finally obtain the electrostatic dispersion relation,

$$1 + \frac{e}{\epsilon_0 k^2}\left(n_e^1 - n_i^1\right)/\Phi^1 = 1 + \chi_e + \chi_i = 0, \tag{18}$$

where ion susceptibility is

$$\chi_i = -\frac{\omega_{pi}^2}{k^2}\frac{(A_i\cdot\vec{k})}{a_i\det A_i}\cdot\frac{(\vec{k}+i\nabla)n^0}{n^0}. \tag{19}$$

With appropriate substitutions we can write down the full dispersion relation as

$$1 - \sum_{l=i,e}\frac{1}{k^2}\frac{\frac{e^2}{\epsilon_0 m_l}(A_l\cdot\vec{k})\cdot(\vec{k}+i\nabla)n^0/\left[(a_l+i\nu_l)\det A_l\right]}{\left[1-\frac{T_l^0}{m_l n^0}\frac{1}{(a_l+i\nu_l)\det A_l}\left\{(A_l\cdot\vec{k})\cdot(\vec{k}+i\nabla)n^0 - \frac{1}{n^0}\left[(iA_l\cdot\nabla n^0)\cdot(\vec{k}+i\nabla)n^0\right]\right\}\right]} = 0, \tag{20}$$

Equation (20) contains all necessary physics to describe oscillations in the thruster discharge, within the limitations described in the beginning of this section. Here through Eqs. (14) and (15) we have introduced the effects of velocity and density gradients. It is interesting to note that while the dispersion relation depends on the magnetic field and temperature, it does not depend explicitly on their gradients. In order to use this dispersion relation one needs to specify profiles of the electric and magnetic fields, electron and ion velocities, plasma density, and electron temperature. These profiles can be either the experimentally measured values or results of a numerical simulation. In case of numerical simulation, the computed $\nu_{AN}$ can be fed back into the solver in order to improve fidelity of the simulation. In case of experimental measurements the dispersion relation can be used to correlate the observed plasma oscillations with anomalous electron mobility.

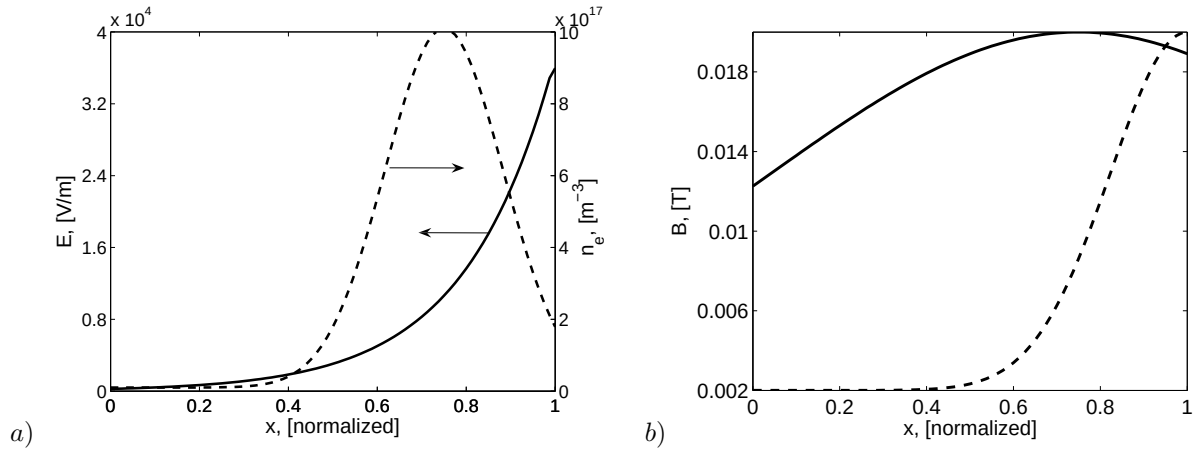


**Figure 2. Zero-order profiles chosen for the investigation of anomalous transport. Anode is located at $x = 0$. Panel a) shows electric field (solid curve) and plasma density (dashed curve) distributions, while panel b) shows two magnetic profiles, one that resembles a realistic HCT magnetic field (dashed curve), and a profile with small magnetic field gradient (solid curve).**

## V. Limiting Case

We now discuss a limiting case in order to check validity of the derived dispersion relation. We will consider a case of collisional, homogeneous, and cold plasma discussed by Litvak and Fisch.[20] We, therefore, set $T_e^0 = 0$, and ignore all gradients. Consequently, $a_{i,e} = b_{i,e}$ and $c_e = d_e$ and we obtain the following dispersion relation,

$$1 - \omega_{pi}^2 \frac{1}{(\omega - k_x v_i^0)^2} - \omega_{pe}^2 \frac{\omega - k_y v_e^0 - i\nu_e}{(\omega - k_y v_e^0)[(\omega - k_y v_e^0 - i\nu_e)^2 - \omega_{ce}^2]} = 0, \tag{21}$$

where $\omega_{pi}$ and $\omega_{pe}$ are the ion and electron plasma frequencies. Following the authors in assuming that $\omega_{ce} \gg |w - k_y v_e^0 - i\nu_e|$, we reproduce the dispersion relation for the lower-hybrid waves, which is modified to include electron collisions, identical to Eq. (16) in Ref. [20]

$$1 - \frac{\omega_{pi}^2}{(\omega - k_x v_i^0)^2} + \frac{\omega_{pe}^2}{\omega_{ce}^2} - \frac{i\nu_e \omega_{pe}^2}{(\omega - k_y v_e^0)\omega_{ce}^2} = 0. \tag{22}$$

Furthermore, assuming a purely azimuthal propagation, the expression above reduces to

$$1 - \frac{\omega_{pi}^2}{\omega^2} + \frac{\omega_{pe}^2}{\omega_{ce}^2} - \frac{i\nu_e \omega_{pe}^2}{(\omega - k_y v_e^0)\omega_{ce}^2} = 0. \tag{23}$$

Had we kept the gradients in the calculations above, we would have gotten a more complicated expression,

$$1 - \frac{\omega_{pi}^2}{\omega(\omega - i\frac{\partial v_i^0}{\partial x})} + \frac{\omega_{pe}^2}{\omega_{ce}^2} - \frac{i\nu_e \omega_{pe}^2}{(\omega - k_y v_e^0 - i\frac{\partial v_e^0}{\partial x})\omega_{ce}^2} + \frac{1}{k_y n^0}\frac{\partial n^0}{\partial x}\frac{\omega_{pe}^2}{(\omega - k_y v_e^0 - i\frac{\partial v_e^0}{\partial x})\omega_{ce}} = 0. \tag{24}$$

We can now proceed to calculate the anomalous collision term for the simple case of the collisional lower-hybrid wave propagating purely in the azimuthal direction. According to Ref. [20] the real and imaginary components of solution to the dispersion relation (23) are

$$\omega_r = \frac{\omega_{pi}\omega_{ce}}{\sqrt{\omega^2 ce + \omega_{pe}^2}} \quad \text{and} \quad \omega_i = \frac{\nu_e}{2k_y v_e^0} \cdot \omega_r. \tag{25}$$

With the assumptions made in the derivation of Eq. (23) the ion susceptibility reduced to

$$\chi_i = \frac{\omega_{pi}^2}{\omega^2}, \tag{26}$$

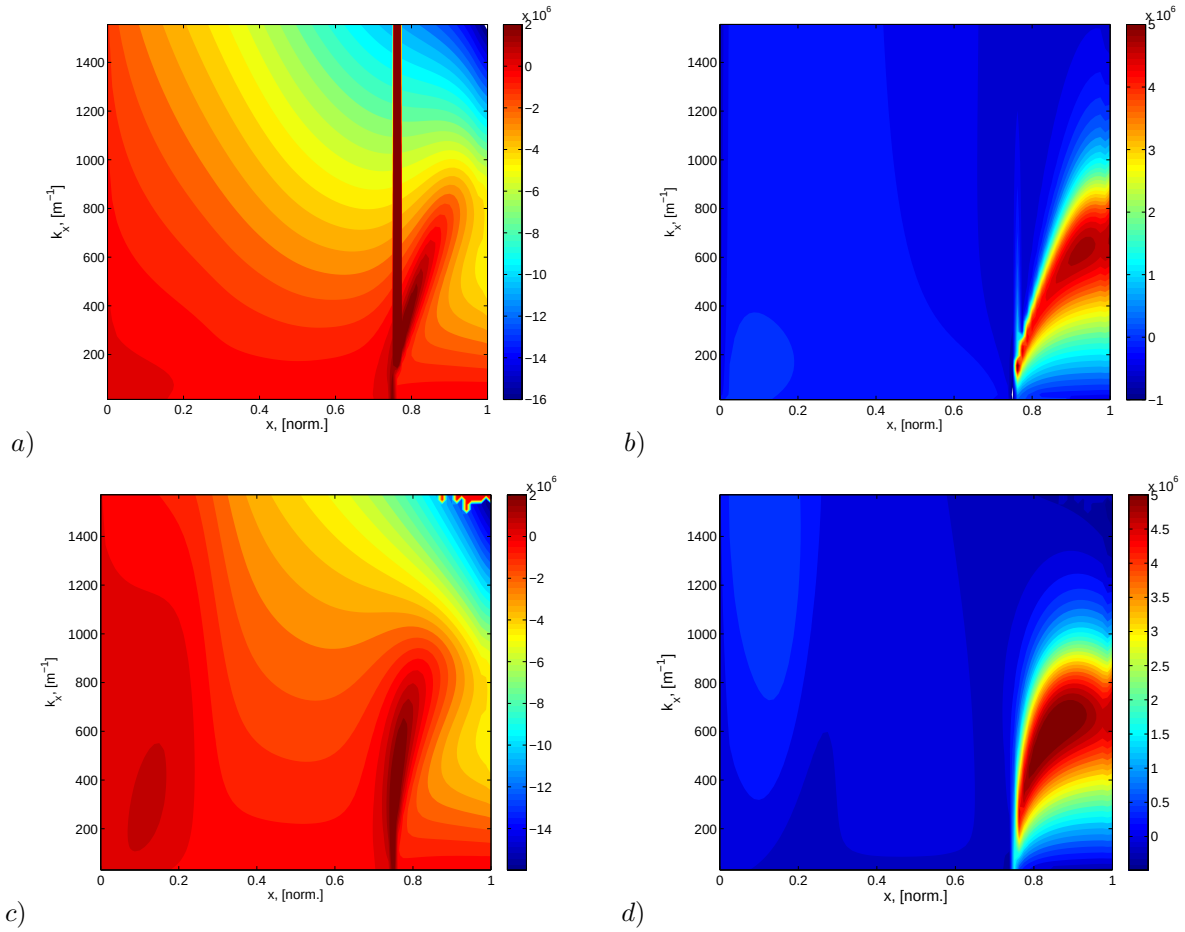


**Figure 3. Real, panels a) and c), and imaginary, panels b) and d), components of solution to dispersion relation with a realistic magnetic field, panels a) and b), and low-gradient magnetic field, panels c) and d).** $m = 1$ **mode.**

which, after some numerical manipulation, leads to

$$\nu_{AN} \sim \frac{1}{\omega_{ce}^2}, \tag{27}$$

where we have also assumed that $\omega_{pe} \gg \omega_{ce}$ and ignored terms not dependent on the magnetic field. Substituting the dependence described by Eq. (27) into expression (4), we see that the anomalous contribution to the total electron mobility scales as $1/B^4$. This scaling is inconsistent with the observed $1/B$ scaling, which is typically attributed to anomalous transport.

## VI. Application to thruster geometry

We now study anomalous transport using Eq. (2) together with Eq. (20) by specifying plasma density, electric field, and magnetic field distributions. The functional form of each of these distributions, shown in Fig. 2, is arbitrary, and was only chosen here for demonstration. While the electric field and plasma density profiles may be representative of a Hall thruster geometry, we set $T_e^0 = 0$, in order to minimize the number of variables. Furthermore, we study two different magnetic field configurations: one with a realistic magnetic field profile, shown by the dashed curve in Fig. 2b), and one with a very week gradient, shown by the solid curve. The latter profile is also shifted slightly toward the anode, to show the effects of location of the maximum magnetic field. In Fig. 2, and following figures, anode is located at $x = 0$, and we also assume that the discharge channel length is $d = 0.04\ m$, while thruster channel mean radius is $r = 0.05\ m$.

We determine the axial and azimuthal electron velocities from these steady state profiles with the help of Eq. (3),

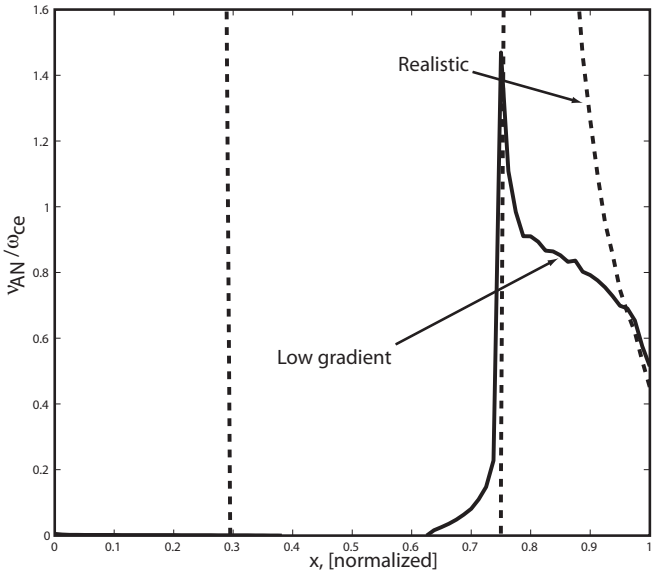


**Figure 4. Anomalous collision frequency ($\nu_{AN}/\omega_{ce}$) profile inside the thruster discharge channel. The dashed curve corresponds to the realistic magnetic field profile, while the solid curve corresponds to the low-gradient profile.**

and assume that the ion flow is purely axial with the following dependence,

$$v_{ix}^0 = \sqrt{\gamma \frac{2e(V_d - \phi)}{m_i}}, \tag{28}$$

where $V_d = 300$ Volt is the total discharge voltage, $\phi$ is the potential at the point where ion velocity is being evaluated, and $\gamma = 3/4$, as discussed in Ref. [9].

The dispersion relation (20) is solved at every position $x$ and with a range of wavenumbers $\vec{k}$ for real and imaginary components of frequency $\omega = \omega_r + i\omega_i$. Values of the wavenumber $\vec{k}$ are chosen with the following restriction. We assume that the azimuthal wavenumber $k_y$ is limited by the radial size of the thruster, and is therefore quantized $k_y = m/r$, where $m$ is the modal number equal to 0,1,2,3, and so on. Here $m = 0$ corresponds to a purely axial wave, and $m \to \infty$ leads to an azimuthal wave. For brevity we will only discuss the $m = 1$ mode.

With this limitation on $k_y$ we let the axial component of the wavelength vary from 0.1 to 10 times the length of the channel. This way we build a two-dimensional solution matrix, shown in Fig. 3. The top two panels of this figure show the real, Fig. 3a), and imaginary, Fig. 3b), components of the frequency as a function of position $x$ along the thruster channel and axial wavenumber $k_x$ for $m = 1$ computed with the realistic magnetic field profile. The bottom two panels of Fig. 3 show similar solutions for the low-gradient magnetic field distribution. It should be noted that for the realistic magnetic field profile the numerical solver we used had trouble finding the right solution at $x \approx 0.8$. Results of this divergence, shown by the vertical red line in Fig. 3a) should not be trusted.

Before we find $\nu_{AN}$ from these solutions, we need to make another simplifying assumption. Figures 3b) and d) show that in the region close to the thruster exit there is a range of wavenumbers, centered at $k_x \sim 600\ \mathrm{m}^{-1}$, with high positive growth rate. This finding implies that a broadband fluctuation ($k_x \sim 400 - 800\ \mathrm{m}^{-1}$) can be excited in the exit region of a Hall thruster. We, however will only seek the maximum growth rate at each $x$, and compute $\nu_{AN}(x)$ based on this single number. A more accurate approach would require integrating over the the full wavenumber range as described by Eq. (2).

We show results of our calculations in Fig. 4 as a ratio of $\nu_{AN}/\omega_{ce}$ at every position in the discharge channel. Here again, results computed with the realistic magnetic field are shown by the dashed curve, while the low-gradient magnetic field profile produces the solid curve. The low-gradient curve shows that anomalous frequency is high in the region close to the thruster exit and falls to zero toward the anode. However, the absolute value of the anomalous collision frequency is an order to two orders of magnitudes too high.[1] Results for the realistic magnetic field case look even less promising. For this case the ratio of the anomalous collision frequency to the electron cyclotron frequency is

$\sim 5$ in the exit region. In addition, close to the anode $\nu_{AN}/\omega_{ce}$ dramatically increases because the cyclotron frequency decreases faster than the anomalous collision frequency.

There are two possible explanations for these discrepant behaviors. First relies on the saturation energy. According to Eq. (2) anomalous frequency is proportional to the energy of saturation. Therefore, if the saturation energy mechanism is less effective than the one we have assumed, the anomalous collision frequency should be lower. However, it is unlikely that the actual saturation energy is two orders of magnitude smaller than the thermodynamic limit that we have assumed.

On the other hand, it is possible that the higher-$m$ modes, have also higher growth rates and, at the same time, lower $\nu_{AN}$, as has been noted in Ref. [15]. Future work will show wether waves propagating at high angles with respect to $x$ (i.e. waves with large $m$) dominate the instability spectrum, producing the observable values of the anomalous electron mobility.

## VII. Conclusions

In this paper we presented a derivation of the anomalous collision frequency inside a Hall thruster discharge based on the quasi-linear approach. The model that we developed calculates effective anomalous electron collision frequency $\nu^{AN}$ from plasma susceptibility, which is computed from the fluid dispersion relation. The dispersion relation was derived in a general form, and incorporates gradients in electric and magnetic fields, as well as electron temperature and density. Additionally, the dispersion relation allows for the wave propagation at an arbitrary direction relative to the applied magnetic field in the $z-\theta$ plane. The gradients can be specified by an analytic expression or as experimentally measured quantities. This makes the derived expression for the anomalous collision frequency a flexible tool that can be used in support of either experimental studies or numerical investigations.

Upon making appropriate approximation, we have shown that the generalized dispersion relation can be reduced to previously published simpler expressions. Furthermore, through an example, we showed how the quasi-linear model can be used to investigate anomalous transport.

## Acknowledgements

The project was supported by The Aerospace Corporation through its Independent Research and Development Program.

## References

[1]Cappelli, M. A., Meezan, N. B., and Gascon, N., "Transport Physics in Hall Plasma Thrusters," Presented at the $40^{th}$ AIAA Aerospace Sciences Meeting and Exhibit, Reno, NV, 14-17, January 2002, AIAA-2003-4701.

[2]Boeuf, J. P. and Garrigues, L., "Low frequency oscillations in a stationary plasma thruster," *J. Appl. Phys.*, Vol. 84, No. 7, October 1998, pp. 3541.

[3]Hagelaar, G. J. M., Bareilles, J., Garrigues, L., and Boeuf, J., "Role of anomalous electron transport in a stationary plasma thruster simulation," *J. Appl. Phys.*, Vol. 93, No. 1, January 2003, pp. 67.

[4]Keidar, M. and Boyd, I., "Modeling of a high-power thruster with anode layer," *Phys. Plasmas*, Vol. 11, No. 4, April 2004, pp. 1715.

[5]Allis, M. K., Gascon, N., and Cappelli, M. A., "Effect of Charge Exchange on 2D Hall Thruster Simulation," Presented at the $29^{th}$ International Electric Propulsion Conference, Princeton University, Princeton, NJ, October 31 November 4, 2005, IEPC-2005-057.

[6]Yoshikawa, S. and Rose, D., "Anomalous Diffusion of a Plasma accross a Magnetic Field," *Phys. Fluids*, Vol. 5, No. 3, March 1962, pp. 334.

[7]Janes, G. and Lowder, R., "Anomalous Electron Diffusion and Ion Acceleration in a Low-Density Plasma," *Phys. Fluids*, Vol. 9, No. 6, June 1966, pp. 1115.

[8]M.Keidar and Beilis, I., "Electron Transport Phenomena in Plasma Devices With $E \times B$ Drift," *IEEE Trans. Plasma Sci.*, Vol. 34, No. 9, June 2006, pp. 804.

[9]Morozov, A. and V.V., S., "Fundamentals of Stationary Plasma Thruster Theory." *Rev. Plasma. Phys.*, Vol. 21, February 2000, pp. 203.

[10]Krall, N. and Book, D., "Ion Sound Instability in a Collisionless Shock Wave," *Phys. Fluids*, Vol. 12, No. 2, February 1969, pp. 347.

[11]Liewer, P. and Krall, N., "Self-consistent approach to anomalous resistivity applied to theta pinch experiments," *Phys. Fluids*, Vol. 16, No. 1, November 1973, pp. 1953.

[12]Rosenberg, M., Krall, N., and McBride, J., "Wave-induced plasma transport in the magnetic drift frequency range," *Phys. Fluids*, Vol. 28, No. 2, November 1984, pp. 538.

[13]Choueiri, E. Y., "Anomalous resistivity and heating in current-driven plasma thrusters," *Phys. Plasmas*, Vol. 6, No. 5, May 1999, pp. 2290.

[14]Choueiri, E. and Spektor, R., "Coherent ion acceleration using two electrostatic waves," Presented at the $36^{th}$ AIAA Joint Propulsion Conference, Huntsville, AL, July 16-20, 2000. AIAA-2000-3759.

[15]Thomas, C. A. and Cappelli, M., "Fluctuation-induced transport in the Hall plasma accelerator," Presented at the $42^{th}$ AIAA/ASME/SAE/ASEE Joint Propulsion Conference (JPC), Sacramento, Ca, 9-12, July 2006, AIAA-2006-5168.

[16]Meezan, N. B. and Cappelli, M. A., "Electron Energy Distribution Function in a Hall Discharge Plasma," Presented at the $37^{th}$ IAIAA/ASME/SAE/ASEE Joint Propulsion Conference, Salt Lake City, Utah, 8-11, July, 2003, AIAA-2001-3326.

[17]Kaganovich, I. D., "Modeling of collisionless and kinetic effects in thruster plasmas," Presented at the $29^{th}$ International Electric Propulsion Conference, Princeton University, Princeton, NJ, October 31 November 4, 2005, IEPC-2005-096.

[18]Kaganovich, I. D., "Kinetic Simulation of Eects of Secondary Electron Emission on Electron Temperature in Hall Thrusters," Presented at the $29^{th}$ International Electric Propulsion Conference, Princeton University, Princeton, NJ, October 31 November 4, 2005, IEPC-2005-078.

[19]Taccogna, F., Schneider, R., Longo, S., and Capitelli, M., "Fully kinetic 2D$r, \theta$ model of a Hall discharge," Presented at the $43^{th}$ AIAA/ASME/SAE/ASEE Joint Propulsion Conference (JPC), Cincinnati, OH, 8 - 11, July 2007, AIAA 2007-5211.

[20]Litvak, A. A. and Fisch, N. J., "Resistive instabilities in Hall current plasma discharge," *Phys. Plasmas*, Vol. 8, No. 2, February 2001, pp. 648.